Mon. Not. R. Astron. Soc. **000**, 1–6 (2009) Printed 24 August 2009 (MN LaTeX style file v2.2)

arXiv:0908.3370v1 [astro-ph.HE] 24 Aug 2009

Global dynamics of advection-dominated accretion flows with magnetically driven outflow

Shuang-Liang Li⋆, Xinwu Cao†
Key Laboratory for Research in Galaxies and Cosmology, Shanghai Astronomical Observatory, Chinese Academy of Sciences,
80 Nandan RD, Shanghai, 200030, China

ABSTRACT

We study the global dynamics of advection-dominated accretion flows (ADAFs) with magnetically driven outflows. A fraction of gases in the accretion flow is accelerated into the outflows, which leads to decreasing of the mass accretion rate in the accretion flow towards the black hole. We find that the r-dependent mass accretion rate is close to a power-law one, $\dot{m}{\propto}r^s$, as assumed in the advection-dominated inflow-outflow solution (ADIOS), in the outer region of the ADAF, while it deviates significantly from the power-law r-dependent accretion rate in the inner region of the ADAF. It is found that the structure of the ADAF is significantly changed in the presence of the outflows. The temperatures of the ions and electrons in the ADAF decreases in the presence of outflows, as a fraction of gravitational power released in the ADAF is tapped to accelerate the outflows.

Key words: accretion, accretion discs – black hole physics – magnetohydrodynamics: MHD – ISM: jets and outflow

1 INTRODUCTION

It is widely believed that many astrophysical objects are powered by mass accretion on to black holes. The standard geometrically thin, optically thick accretion disc model can successfully explain most of the observational features in active galactic nuclei (AGN) and X-ray binaries (Shakura & Sunyaev 1973). In the standard thin model, the motion of the matter in the accretion disc is nearly Keplerian, and the gravitational energy released in the disc is radiated away locally. An alternative accretion disc model, namely, the advection-dominated accretion flow (ADAF) model, was suggested for the black holes accreting at very low rates (Ichimaru 1977; Narayan & Yi 1994). In the ADAF model, only a small fraction of the gravitational energy released in the accretion flow is radiated away due to inefficient cooling, and most of the energy is stored in the accretion flow and advected to the black hole. The ADAFs are optically thin and hot (comparable with the virial temperature of the gases in the flows), which radiate mostly in X-ray waveband (see Narayan & McClintock 2008, for a review and references therein). This model can successfully explain the main observational features of black hole X-ray binaries and low-luminosity AGN (LLAGN) (e.g., Narayan & Yi 1994, 1995a; Gammie et al. 1999; Quataert et al. 1999; Yuan et al. 2003; Ho 2008). As the Bernoulli parameter of an ADAF is positive, the ADAF is likely to have an outflow, which was confirmed by numerical simulations and also supported by observations (Stone & Pringle 2001; Igumenshchev et al. 2003; McKinney 2006; Gammie et al. 1999; Quataert et al. 1999; Yuan et al. 2003).

Blandford & Begelman (1999) proposed a self-similar advection-dominated inflow-outflow solution (ADIOS) for the ADAF with winds. In ADIOS model, the mass accretion rate is no longer a constant and is assumed to be a power-law dependence of radius ($\dot{m} \propto r^s, 0 < s < 1$), which is an important ingredient in most of the follow-up works (e.g., Quataert & Narayan 1999; Yuan et al. 2003; Xue & Wang 2005). Motivated by the results of numerical simulations on accretion discs, Xie & Yuan (2008) investigated the influence of outflows on the accretion flow based on a 1.5-dimensional description of the accretion flow. They suggested that their solutions can be described by a power-law r-dependent mass accretion rate fairly well.

Magnetic fields are believed in accretion flows, and the magnetorotational instability (MRI) provides the source of viscosity in accretion flows (Balbus & Hawley 1991, 1998). The outflows/jets can be driven by the large-scale ordered magnetic fields threading the accretion disc (Blandford & Payne 1982). The physics of magnetically accelerated outflows has been extensively explored in many previous works (e.g., Cao & Spruit 1994; Cao 2002; Kudoh & Shibata 1995; Koide, Shibata, & Kudoh 1999; Kato, Kudoh, & Shibata 2002; Ogilvie & Livio 1998, 2001; Narayan, McKinney, & Farmer 2007; McKinney & Narayan 2007a,b). Such outflows/jets magnetically driven from the accretion discs provide an efficient angular momentum loss mechanism for accretion discs (see Spruit 2008, for a review and references therein). The structure of a standard thin disc/ADAF may be altered by the magnetically driven outflows (e.g., Li, Wang, & Gan 2008;

⋆ E-mail:lisl@shao.ac.cn
† E-mail:cxw@shao.ac.cn

Li, Gan, & Wang 2009). In this work, we investigate the global structure of an ADAF with magnetically driven outflows/jets.

2 MODEL

We consider a steady ADAF with magnetically driven outflows/jets surrounding a black hole in this work.

The continuity equation is

$$\frac{d}{dR}(2\pi R\Sigma v_{\rm R})+4\pi R\dot{m}_{\rm w}=0, \tag{1}$$

where $v_{\rm R}$ is the radial velocity, $\Sigma=2H\rho$ is the surface density of the accretion flow, and $\dot{m}_{\rm w}$ is the mass loss rate from unit surface area of accretion flow. The half-thickness of the disc H is given by $H=c_{\rm s}/\Omega_{\rm K}$, and $\Omega_{\rm K}$ is the Keplerian angular velocity. The sound speed $c_{\rm s}=(P/\rho)^{1/2}$, and the total pressure P is the sum of the gas pressure and the magnetic pressure: $P=P_{\rm gas}+P_{\rm m}=P_{\rm i}+P_{\rm e}+P_{\rm m}$ ($P_{\rm i}$ and $P_{\rm e}$ are the ion pressure and the electron pressure respectively).

In this work, we adopt the Paczyński–Wiita potential

$$\psi=-\frac{GM}{R-R_{\rm g}} \tag{2}$$

to simulate the general relativistic effects of a Schwarzschild black hole, where M is the mass of the black hole, and $R_{\rm g}=2GM/c^2$ is the gravitational radius (Paczyński & Wiita 1980).

The radial momentum equation is

$$v_{\rm R}\frac{dv_{\rm R}}{dR}-R(\Omega^2-\Omega_{\rm K}^2)+\frac{1}{\rho}\frac{dP}{dR}-g_{\rm m}=0, \tag{3}$$

where Ω is the angular velocity of the accretion flow. The radial magnetic force is given by

$$g_{\rm m}=\frac{B_{\rm r}^{\rm s}B_{\rm z}}{2\pi\Sigma}, \tag{4}$$

where $B_r^{\rm s}$ and B_z are the radial and vertical components of the magnetic fields at the disc surface.

The angular momentum equation reads

$$v_R\frac{d(\Omega R^2)}{dR}-\frac{1}{\rho HR}\frac{d}{dR}(R^2H\tau_{r\varphi})+\frac{T_{\rm m}}{\Sigma}=0, \tag{5}$$

where α-viscosity $\tau_{r\varphi}=-\alpha P$ is adopted (Shakura & Sunyaev 1973), and $T_{\rm m}$ is the magnetic torque exerted on the accretion flow due to the outflows/jets. The outflow is accelerated by the magnetic fields threading the rotating accretion disc, and therefore the torque $T_{\rm m}$ can be calculated with

$$T_{\rm m}=2\dot{m}_{\rm w}\Omega(R_{\rm d})(R_{\rm A}^2-R_{\rm d}^2), \tag{6}$$

where $\dot{m}_{\rm w}$ is the mass loss rate due to the outflow, $R_{\rm d}$ is the radius of the footpoint of the field line, and $R_{\rm A}$ is the Alfvén point (see, e.g., Cao 2002, for the details).

The energy equations for ions and electrons are given by

$$\rho v_R\Big(\frac{d\varepsilon_{\rm e}}{dR}-\frac{P_{\rm e}}{\rho^2}\frac{d\rho}{dR}\Big)-\delta q^+-q_{\rm ie}+q^-+\frac{2\dot{m}_{\rm w}\varepsilon_{\rm e}}{2H}=0, \tag{7}$$

and

$$\rho v_{\rm R}\Big(\frac{d\varepsilon_{\rm i}}{dR}-\frac{P_{\rm i}}{\rho^2}\frac{d\rho}{dR}\Big)-(1-\delta)q^++q_{\rm ie}+\frac{2\dot{m}_{\rm w}\varepsilon_{\rm i}}{2H}=0, \tag{8}$$

respectively, where the parameter δ describes the fraction of the viscously dissipated energy that goes directly into electrons in the accretion flow, and the specific internal energy of electrons and ions are given by

$$\varepsilon_{\rm e}=\frac{1}{\gamma_{\rm e}-1}\frac{kT_{\rm e}}{\mu_{\rm e}m_{\rm H}}, \tag{9}$$

$$\varepsilon_{\rm i}=\frac{1}{\gamma_{\rm i}-1}\frac{kT_{\rm i}}{\mu_{\rm i}m_{\rm H}}, \tag{10}$$

where $T_{\rm e}$ and $T_{\rm i}$ are the temperature of electrons and ions respectively, and the mean molecular weight of the ions and the electrons: $\mu_{\rm i}=1.23$, $\mu_{\rm e}=1.14$ are adopted. The adiabatic indices of the electrons and ions, $\gamma_{\rm e}$ and $\gamma_{\rm i}$, are given by

$$\gamma_{\rm e}=1+\theta_{\rm e}\left[\frac{3K_3(1/\theta_{\rm e})+K_1(1/\theta_{\rm e})}{4K_2(1/\theta_{\rm e})}-1\right]^{-1}, \tag{11}$$

$$\gamma_{\rm i}=1+\theta_{\rm i}\left[\frac{3K_3(1/\theta_{\rm i})+K_1(1/\theta_{\rm i})}{4K_2(1/\theta_{\rm i})}-1\right]^{-1}, \tag{12}$$

where $K's$ are the modified Bessel functions, and the dimensionless electron and ion temperature are defined as: $\theta_{\rm e}=kT_{\rm e}/(m_{\rm e}c^2)$ and $\theta_{\rm i}=kT_{\rm i}/(m_{\rm p}c^2)$ (Narayan & Yi 1995b). The energy dissipation rate per unit volume is given by $q^+=-\alpha PRd\Omega/dR$, and $q_{\rm ie}$ indicates the energy transfer rate from ions to electrons through Coulomb collisions, which is given by (Stepney & Guilbert 1983)

$$q_{\rm ie}=\frac{3}{2}\frac{m_{\rm e}}{m_{\rm p}}n_{\rm e}n_{\rm i}\sigma_{\rm T}c\frac{(kT_{\rm i}-kT_{\rm e})}{K_2(1/\theta_{\rm e})K_2(1/\theta_{\rm i})}{\rm ln}\Lambda$$

$$\times\left[\frac{2(\theta_{\rm e}+\theta_{\rm i})^2+1}{(\theta_{\rm e}+\theta_{\rm i})}K_1\left(\frac{\theta_{\rm e}+\theta_{\rm i}}{\theta_{\rm e}\theta_{\rm i}}\right)+2K_0\left(\frac{\theta_{\rm e}+\theta_{\rm i}}{\theta_{\rm e}\theta_{\rm i}}\right)\right], \tag{13}$$

where the Coulomb logarithm ${\rm ln}\Lambda=20$, and q^- is the radiative cooling rate consisting of synchrotron, bremsstrahlung, and Compton cooling (see, Narayan & Yi 1995b; Manmoto 2000, for details).

The dynamical properties of magnetically driven outflows/jets from an accretion disk can be investigated by solving a set of magneto-hydrodynamical (MHD) equations if the magnetic field configuration of the disk and suitable boundary conditions at the disk surface are supplied (e.g., Cao & Spruit 1994; Cao 2002; Kudoh & Shibata 1995; Koide, Shibata, & Kudoh 1999; Kato, Kudoh, & Shibata 2002; Ogilvie & Livio 1998, 2001). However, the generation and maintenance of large-scale magnetic fields of the disk is still quite unclear (e.g., Lubow, Papaloizou, & Pringle 1994a,b; Tout & Pringle 1996). In this work, we focus on how the dynamics of the ADAF is affected by the presence of magnetically driven outflows/jets. For simplicity, we assume that large-scale magnetic field lines thread the accretion disk, and the strength of the magnetic fields far from the disc surface along the field line to be roughly self-similar:

$$B_{\rm p}(R)\sim B_{\rm pd}\left(\frac{R}{R_{\rm d}}\right)^{-\zeta}, \tag{14}$$

where $R_{\rm d}$ is the radius of the field footpoint at the disc surface, $B_{\rm pd}$ is the strength of the poloidal component of the field at the disc surface, $B_{\rm p}(R)$ is the field strength at R along the field line, the self-similar index $\zeta\geqslant 1$ (Blandford & Payne 1982), and $\zeta=4$ is adopted in the calculations of Lubow, Papaloizou, & Pringle (1994b).

The self-similar wind solution derived by Lubow, Papaloizou, & Pringle (1994b) is only valid for slowly moving (non-relativistic) outflows, which was extended for relativistic jets by Cao (2002). In this work, we model the magnetically driven outflows/jets with the approach adopted in Cao (2002). We summarize the model as follows (see Cao 2002, for the details).

For a relativistic jet accelerated by the magnetic field of the disc, the Alfvén velocity is (Michel 1969; Camenzind 1986)

$$v_{\rm A}=\frac{B_{\rm p}^{\rm A}}{(4\pi\rho_{\rm A}\gamma_{\rm j})^{1/2}}, \tag{15}$$

where $B_{\rm p}^{\rm A}$ and $\rho_{\rm A}$ are the poloidal field strength and the density of the outflow/jet at Alfvén point, and $\gamma_{\rm j}$ is the Lorentz factor of the bulk motion of the outflows/jets. In this work, all our calculations of the outflows/jets are in the special relativistic frame. The Alfvén velocity $v_{\rm A}\sim R_{\rm A}\Omega(R_{\rm d})$, where $R_{\rm A}$ is the radius of the Alfvén point along the field line, and $\Omega(R_{\rm d})$ is the angular velocity of the accretion flow at the field footpoint $R_{\rm d}$.

The mass and magnetic flux conservation along the field line requires

$$\frac{\dot m_{\rm w}}{B_{\rm pd}}\simeq\frac{\rho_{\rm A}v_{\rm A}}{B_{\rm p}^{\rm A}}, \tag{16}$$

where $\dot m_{\rm w}$ is the mass loss rate in the outflow/jet from unit surface area of the disc.

The final bulk velocity of the magnetically driven outflow/jet is $\sim v_{\rm A}$, so the Lorentz factor of the outflow/jet is

$$\gamma_{\rm j}\simeq\left[1-\left(\frac{v_{\rm A}}{c}\right)^2\right]^{-\frac{1}{2}}. \tag{17}$$

Combining equations (14)–(17), the mass loss rate in the outflow/jet from the unit surface area of the disc is

$$\dot m_{\rm w}=\frac{B_{\rm pd}^2}{4\pi c}\left[\frac{R_{\rm d}\Omega(R_{\rm d})}{c}\right]^{\zeta}\frac{\gamma_{\rm j}^{\zeta}}{(\gamma_{\rm j}^2-1)^{(1+\zeta)/2}}. \tag{18}$$

The origin of the ordered magnetic fields threading the disc is still unclear. It was suggested that the magnetic fields can be generated through dynamo processes in the disc (e.g., Shakura & Sunyaev 1973; Tout & Pringle 1996; Armitage 1998; Romanova et al. 1998), or the large-scale external magnetic fields are transported inward by the accretion flow (e.g., Bisnovatyi-Kogan & Ruzmaikin 1976; Lubow, Papaloizou, & Pringle 1994a; Spruit & Uzdensky 2005). For simplicity, we assume the strength of the large-scale magnetic fields threading the disc to be comparable with that of the fields in the accretion disc, $B_{\rm pd}\simeq B$. The magnetic pressure is conventionally assumed to be proportional to the gas pressure in the accretion flow. Thus, we have

$$P_{\rm m}=\frac{B^2}{8\pi}=\frac{1-\beta}{\beta}P_{\rm gas}, \tag{19}$$

where β is the ratio of the gas pressure to the total pressure, B is the strength of the magnetic fields in the accretion flow.

The magnetically driven outflow is described by the terminal velocity of the outflow (Alfvén velocity $v_{\rm A}$) when the values of two parameters ζ and β are specified.

3 RESULTS

We use the Runge-Kutta method to solve a set of five differential equations (1),(3),(5),(7) and (8) for five variables: ρ, $v_{\rm R}$, Ω, $T_{\rm e}$ and $T_{\rm i}$ with suitable boundary conditions at the outer radius $R_{\rm out}$. In our calculations, we adopt the black hole mass $M=10^8M_{\odot}$ for a typical AGN. The conventional values of the disc parameters: $\alpha=0.1$ and $\delta=0.1$, are adopted in all our calculations. The temperature of the ADAF at the outer radius is adopted as described by the self-similar solution of Narayan & Yi (1995b). We use a shooting point method in our calculations. Integrating these five equations from the outer boundary of the flow at $R=R_{\rm out}$ inwards toward the black hole, we can obtain the global structure of the accretion flow passing the sonic point smoothly to the black hole horizon by tuning the value of radial velocity at $R_{\rm out}$. The outer radius of the accretion flow $R_{\rm out}=5000R_{\rm g}$ is adopted. We find that the structure of the ADAF is insensitive to the outer boundary conditions. As discussed in Sect. 2, the magnetically driven outflow is described by $v_{\rm A}$, ζ and β. The terminal bulk velocity of the outflow is comparable with the Alfén velocity $v_{\rm A}$. For any unbounded outflows, its bulk velocity should $\gtrsim v_{\rm K}$, which implies $v_{\rm A}\gtrsim v_{\rm K}$.

The mass accretion rate at the outer radius, $\dot M=10^{-5}\dot M_{\rm Edd}$ (the Eddington rate is defined as $\dot M_{\rm Edd}=1.5\times10^{18}M/{\rm M}_{\odot}$ g s^{-1}), is adopted for the calculations plotted in Figs. 1– 3. In Fig. 1, the global solutions for the ADAFs with outflows are shown with different magnetic field strengths and distributions (i.e., different values of β and ζ), in which $v_{\rm A}=v_{\rm K}$ is adopted. In the left panel of Fig. 1, the radial velocity and the sound speed as functions of radius with different values of β are plotted for $\zeta=1$. In the right panel of Fig. 1, the mass accretion rates as functions of radius are plotted for the global solutions with different values of β and ζ.

In Fig. 2, we plot different quantities of ADAF solutions with $\zeta=1$ and 4, respectively, where $v_{\rm A}=v_{\rm K}$ and $\beta=0.9$ are adopted. As comparison, we also plot the ADAF solutions without outflows in the same figure. In the calculations, the terminal velocity of the outflow is a free parameter. We compare the global ADAF solutions with different values of $v_{\rm A}$ (i.e., $v_{\rm A}=v_{\rm K}$ and $v_{\rm A}=2v_{\rm K}$) in Fig. 3 with $\beta=0.9$ and $\zeta=1$. In Figs. 4–6, we plot the results calculated with a relatively high mass accretion rate, $\dot m_0=10^{-2}$, at the outer radius of the disc.

The ratio of the bolometric luminosity of accretion disc $L_{\rm bol}$ to kinetic power of outflows $P_{\rm k,w}$ is calculated with

$$\frac{L_{\rm bol}}{P_{\rm k,w}}=\int_{R_{\rm in}}^{R_{\rm out}}q^{-}4\pi RH{\rm d}R\Big/\int_{R_{\rm in}}^{R_{\rm out}}(\gamma_{\rm j}-1)\dot m_{\rm w}c^2 4\pi R{\rm d}R. \tag{20}$$

We plot the ratio $L_{\rm bol}/P_{\rm k,w}$ as functions of magnetic field strength β in Fig. 7, where $v_{\rm A}=v_{\rm K}$ is adopted.

4 DISCUSSION

A fraction of gases in accretion flow is carried away by the magnetically driven outflow, which leads to mass accretion rate of the accretion flow decreasing towards the black hole. In many previous works, the outflow is induced by assuming the mass accretion rate $\dot m$ to be a power-law dependence of radius $\dot m\propto r^s$ (e.g., Blandford & Begelman 1999). In this work, we obtain global solutions of ADAFs with magnetically driven outflows. Our results show that the mass accretion rate $\dot m$ decreases towards the black hole, which is close to a power-law r-dependence at larger radii, while it deviates from a power-law r-dependence in the inner region of the ADAF close to the black hole (see Figs. 1 and 4). The large-scale magnetic fields are assumed to thread the accretion flow, which are believed to accelerate the outflow from the accretion disc. In this work, the magnetic strength at the disc surface is described by a parameter β, which is limited by the gas pressure in the accretion flow. For comparison, we also plot power-law r-dependent accretion rates in Fig. 1. Our calculations show that the mass loss rate in the outflow cannot be very high even if the magnetic fields of the ADAF are very strong (see Fig. 1), i.e., the mass loss rate in the outflow is less than a power-law r-dependent accretion rate with $s\lesssim0.73$. We also calculate the cases with high accretion rate, $\dot m=10^{-2}$, at the outer radius. It is found that the results are qualitatively similar to those with $\dot m=10^{-5}$.

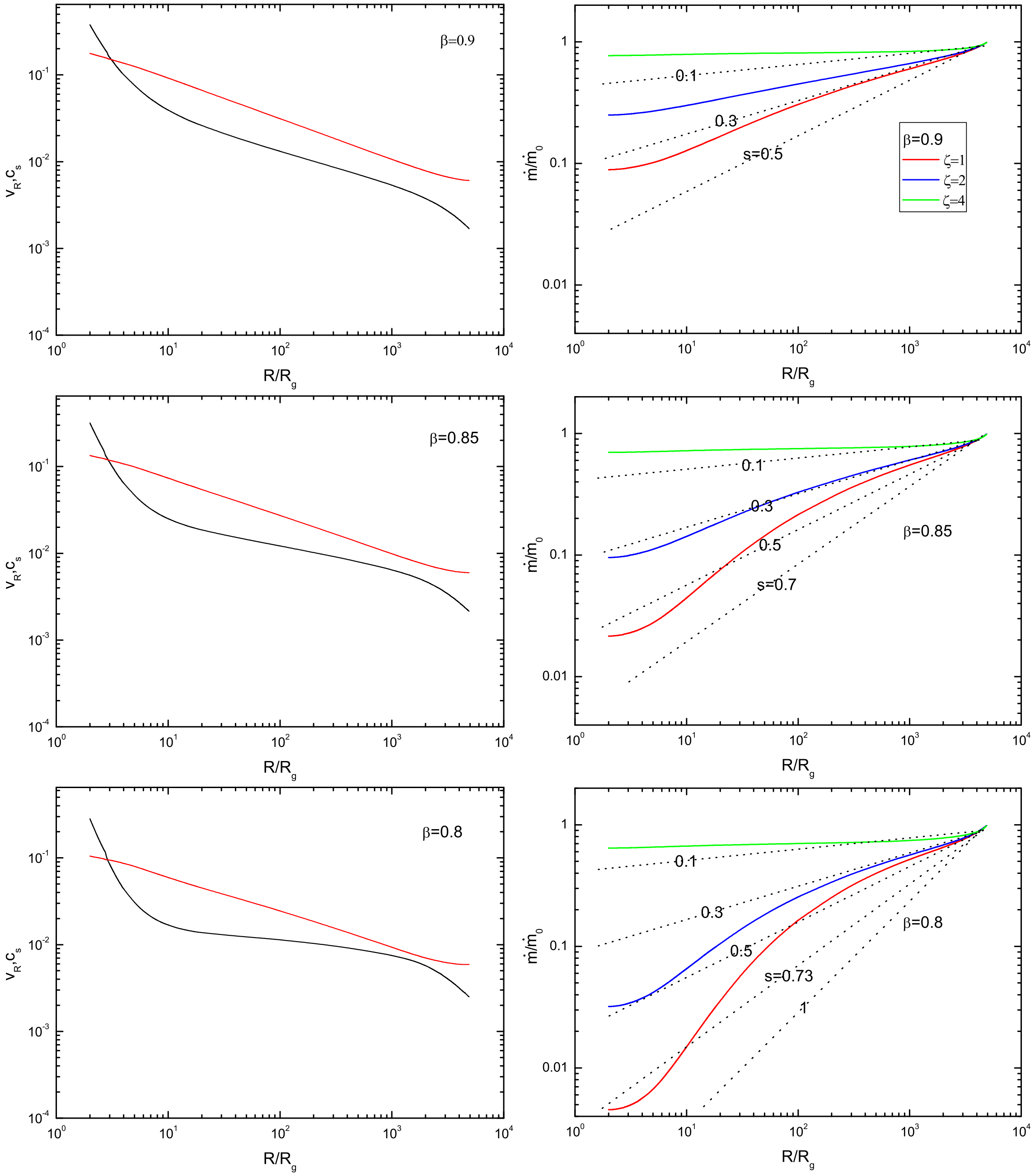

Figure 1. The global solutions of ADAFs with magnetically driven outflows with different parameters. The black and red lines in the left figures are for the radial velocity $v_{\rm R}$ and the sound speed $c_{\rm s}$ respectively. The dotted lines represent power-law r-dependent mass accretion rates with different values of s. The accretion rate at the outer radius ($r_{\rm out}=5000$) is: $\dot{m}_0=10^{-5}$.

For the ADAFs with magnetically driven outflows, the structure of the accretion flow is significantly altered in the presence of the outflow. We find that both the ion and electron temperatures of the ADAF decrease with increasing mass loss rate in the outflow (see Figs. 2 and 3). This is due to the fact that a fraction of the gravitational energy released in the accretion flow is tapped to accelerate the outflow, which decreases the heating of the ADAF. It is easy to understand that the ratio $L_{\rm bol}/P_{\rm k,w}$ increases with decreasing magnetic field strength (see Fig. 7). Based on the magnetically driven outflow model described in Sect. 2, the kinetic power of the outflow $P_{\rm k,w}$ can be estimated with

$$P_{\rm k,w}\propto\frac{1}{2}\dot{m}_{\rm w}v_{\rm A}^2\propto\frac{(R\Omega)^{\zeta}}{v_{\rm A}^{\zeta-1}}, \qquad (21)$$

in the non-relativistic limit. It is found that the kinetic power of the outflow decreases with increasing terminal outflow velocity, which leads to the structure (e.g., temperatures) of ADAFs is less altered by the outflows with higher terminal velocity (see Figs. 3 and 6).

In our present calculations, the magnetic field strength is estimated with the gas pressure in the ADAF, which is true for the fields generated with dynamo processes (see, e.g., the discussion in Livio et al. 1999). In this work, the fields are implicitly assumed to be balanced between diffusion and dynamo/inward advection in

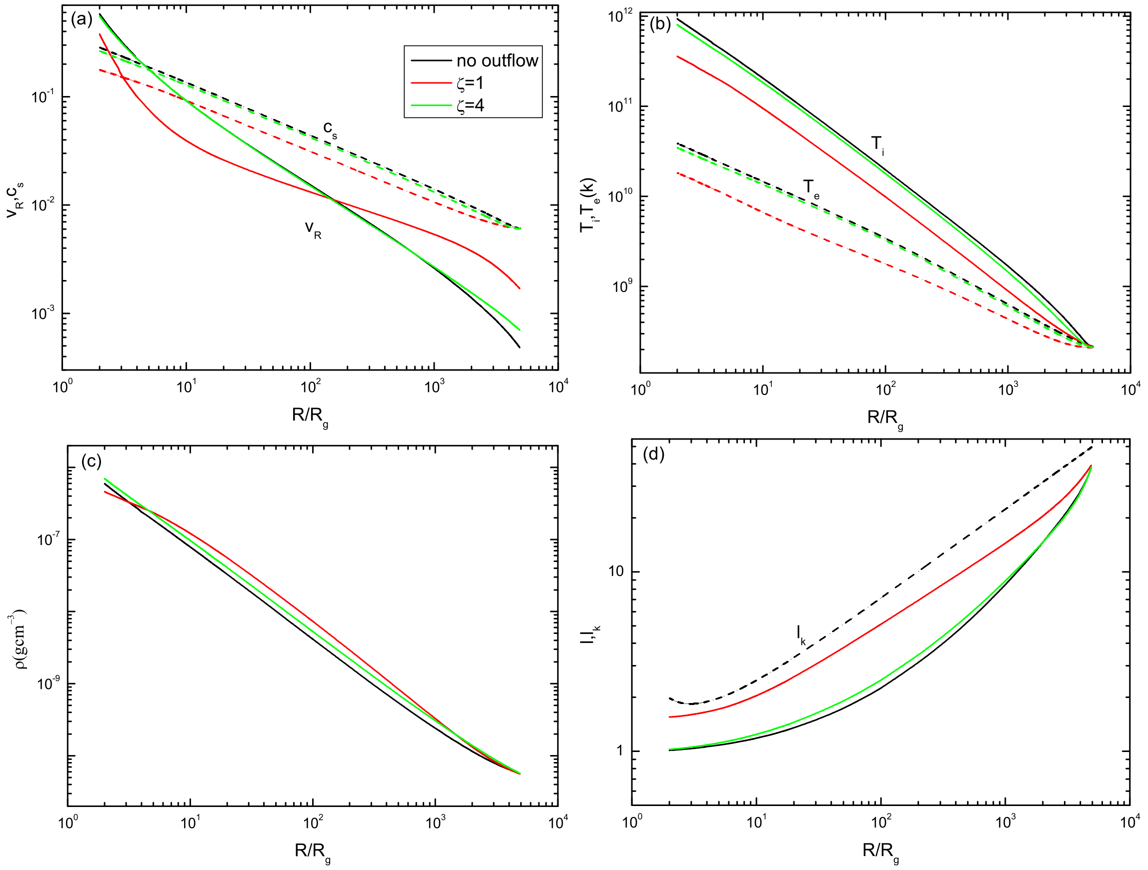

Figure 2. The global structures of ADAFs with magnetically driven outflows. We also plot the structures of ADAFs without outflows for comparison (black lines).

our calculations. The ordered magnetic fields may be maintained by the drag-in process in the accretion disc, in which the magnetic field strength is determined by the balance of the advection and diffusion of the fields in the disc (e.g., Lubow, Papaloizou, & Pringle 1994a). The magnetic fields can therefore be stronger than the equipartition limit, however, the detailed physics is still quite unclear (e.g., Lubow, Papaloizou, & Pringle 1994b; Cao & Spruit 2002; Spruit & Uzdensky 2005; Guan & Gammie 2009). In this case, the value β (see Eq. 19) describing the magnetic field strength may vary with radius, which is determined by the balance between the diffusion and advection of the fields in the accretion flow (e.g., Lubow, Papaloizou, & Pringle 1994b). The mass loss rate in the outflow can be higher than the results presented in this work, if the advection of the magnetic fields by the accretion flow is dominant over the diffusion in the disc.

ACKNOWLEDGEMENTS

This work is supported by the NSFC (grants 10773020, 10821302 and 10833002), the CAS (grant KJCX2-YW-T03), and the National Basic Research Program of China (grant 2009CB824800). S.-L. Li thanks the support from the Knowledge Innovation Program of Chinese Academy of Sciences.

REFERENCES

Armitage P. J., 1998, ApJ, 501, L189
Balbus, S., & Hawley, J. F. 1991, ApJ, 376, 214
Balbus, S., & Hawley, J. F. 1998, RvMP, 70, 1
Bisnovatyi-Kogan G. S., Ruzmaikin A. A., 1976, Ap&SS, 42, 401
Blandford, R. D., & Begelman, M. C. 1999, MNRAS, 303, L1
Blandford, R. D., & Payne, D. G. 1982, MNRAS, 199, 883
Camenzind M. 1986, A&A, 156, 137
Cao, X., 2002, MNRAS, 332, 999
Cao X., Spruit H. C., 1994, A&A, 287, 80
Cao, X., & Spruit H.C. 2002, A&A, 385, 289
Gammie, C. F., Narayan, R., & Blandford, R. D. 1999, ApJ, 516, 177
Guan X., Gammie C. F., 2009, arXiv, arXiv:0903.3757
Ho, L. C. 2008, ARA&A, 46, 475
Ichimaru S., 1977, ApJ, 214, 840
Igumenshchev, I. V., Narayan, R., & Abramowicz, M. A. 2003, ApJ, 592, 1042
Kato S. X., Kudoh T., Shibata K., 2002, ApJ, 565, 1035
Koide S., Shibata K., Kudoh T., 1999, ApJ, 522, 727
Kudoh T., Shibata K., 1995, ApJ, 452, L41
Li Y., Gan Z. M., Wang D. X., New Astron., submitted
Li Y., Wang D.-X., Gan Z.-M., 2008, A&A, 482, 1
Livio, M., Ogilvie, G. I., & Pringle, J. E. 1999, ApJ, 512, 100
Lubow S. H., Papaloizou J. C. B., Pringle J. E., 1994, MNRAS, 267, 235
Lubow S. H., Papaloizou J. C. B., Pringle J. E., 1994, MNRAS,

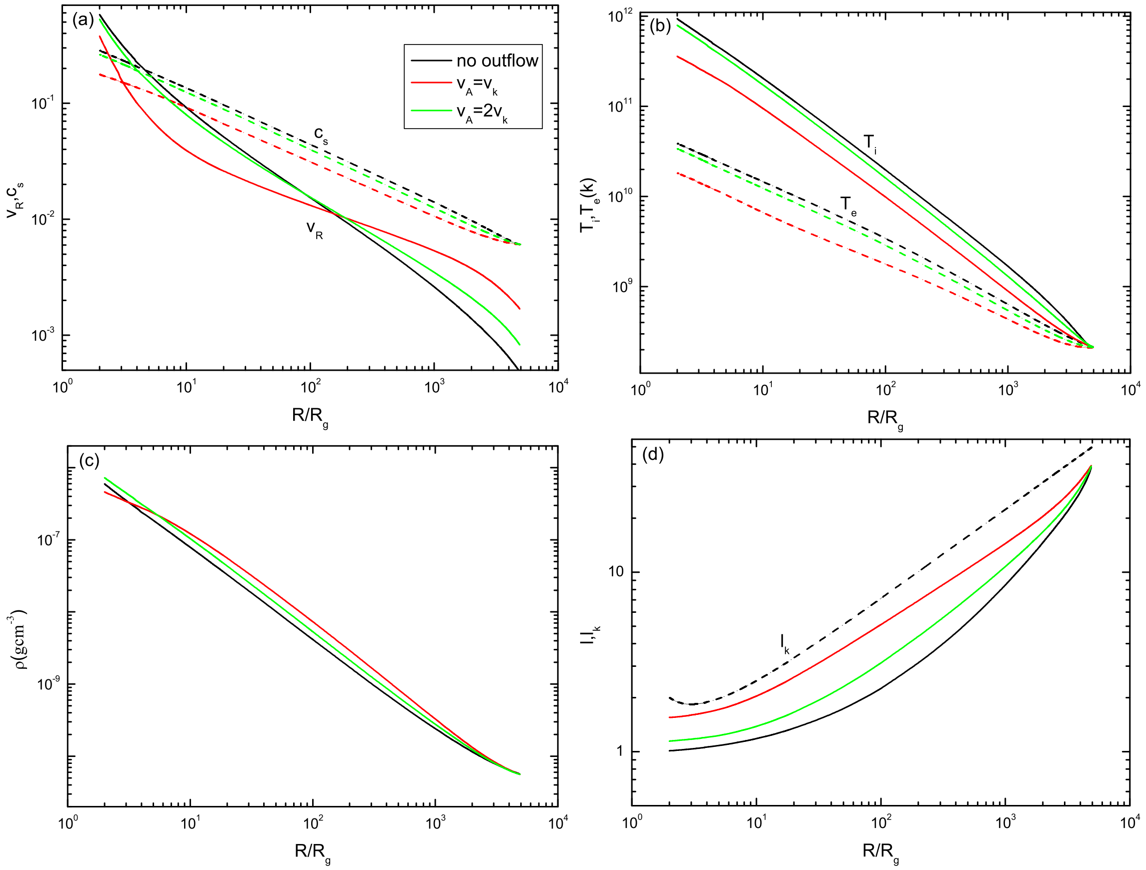

Figure 3. The comparison of global structures of ADAFs with different terminal velocities of the outflows. We also plot the structures of ADAFs without outflows for comparison (black lines).

268, 1010
Manmoto T. 2000, ApJ, 534, 734
McKinney, J. C. 2006, MNRAS, 368, 1561
Michel F. C., 1969, ApJ, 158, 727
McKinney J. C., Narayan R., 2007a, MNRAS, 375, 513
McKinney J. C., Narayan R., 2007b, MNRAS, 375, 531
Narayan R., McClintock J. E., 2008, NewAR, 51, 733
Narayan R., McKinney J. C., Farmer A. J., 2007, MNRAS, 375, 548
Narayan, R., & Yi, I. 1994, ApJ, 428, L13
Narayan, R., & Yi, I. 1995a, ApJ, 444, 231
Narayan, R., & Yi, I. 1995b, ApJ, 452, 710
Ogilvie G. I., Livio M., 1998, ApJ, 499, 329
Ogilvie G. I., Livio M., 2001, ApJ, 553, 158
Paczyński, B., & Wiita, P. J. 1980, A&A, 88, 23
Quataert, E., Di Matteo, T., Narayan R., & Ho, L. C., 1999, ApJ, 525, L89
Quataert, E., & Narayan, R. 1999, ApJ, 520, 298
Romanova M. M., Ustyugova G. V., Koldoba A. V., Chechetkin V. M., Lovelace R. V. E., 1998, ApJ, 500, 703
Shakura, N. I., & Sunyaev, R. A. 1973, A&A, 24, 337
Spruit, H. C. 1996, in Physical Processes in Binary Stars, ed. R. A. M. J. Wijers, M. B. Davis, & C. A. Tout (Kluwer Dordrecht), 249
Spruit H. C., 2008, arXiv, arXiv:0804.3096
Spruit H. C., Uzdensky D. A., 2005, ApJ, 629, 960
Stepney, S., & Guilbert, P. W. 1983, MNRAS, 204, 1269
Stone, J. M., & Pringle, J. E. 2001, MNRAS, 322, 461
Tout C. A., Pringle J. E., 1996, MNRAS, 281, 219
Xie, F. G., & Yuan, F. 2008, ApJ, 681, 499
Xue, L., & Wang, J. 2005, ApJ, 623, 372
Yuan, F., Quataert, E., & Narayan, R. 2003, ApJ, 598, 301

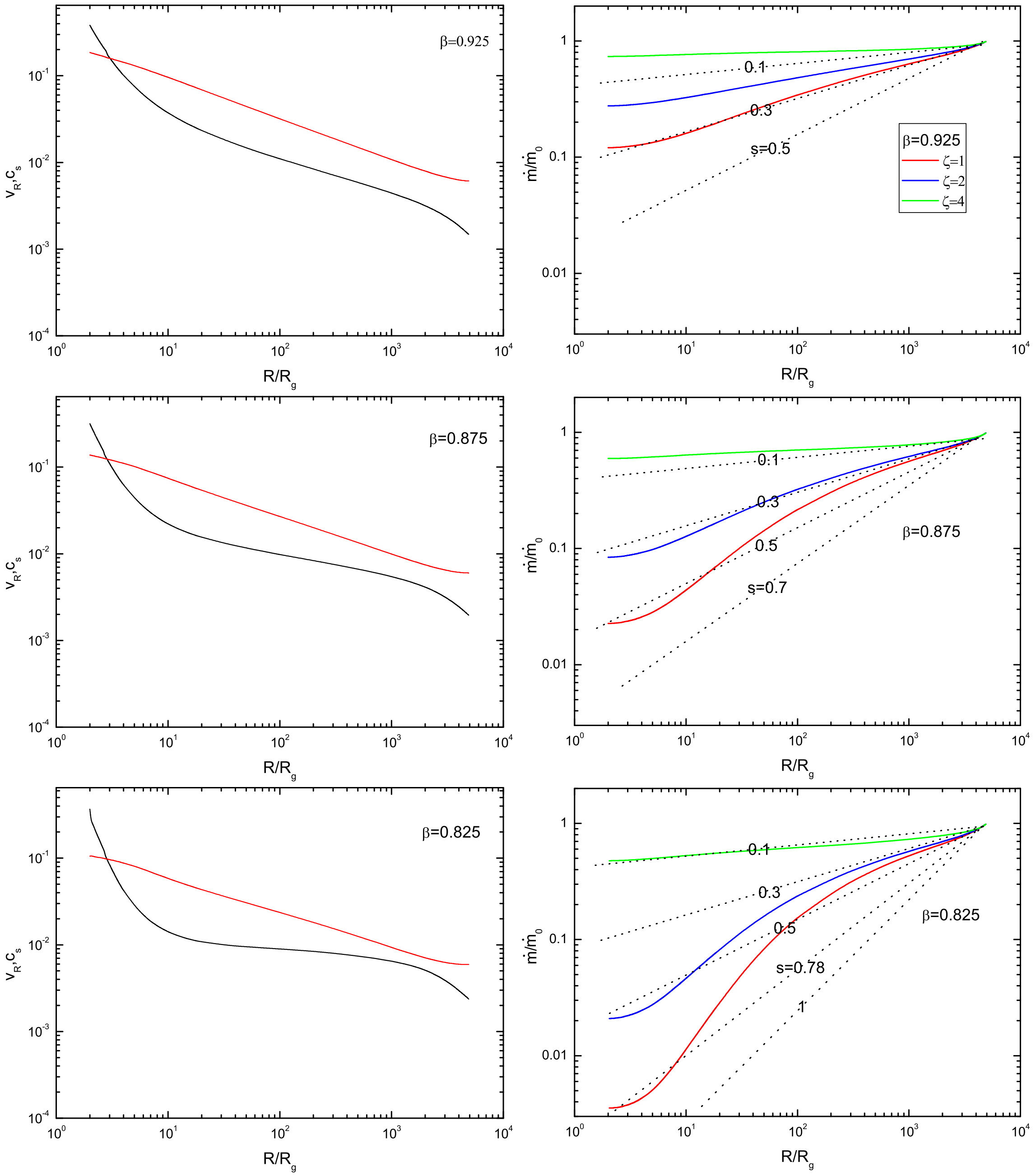

Figure 4. The same as Fig. 1, but the accretion rate at the outer radius, $\dot{m}_0 = 10^{-2}$, is adopted in the calculations.

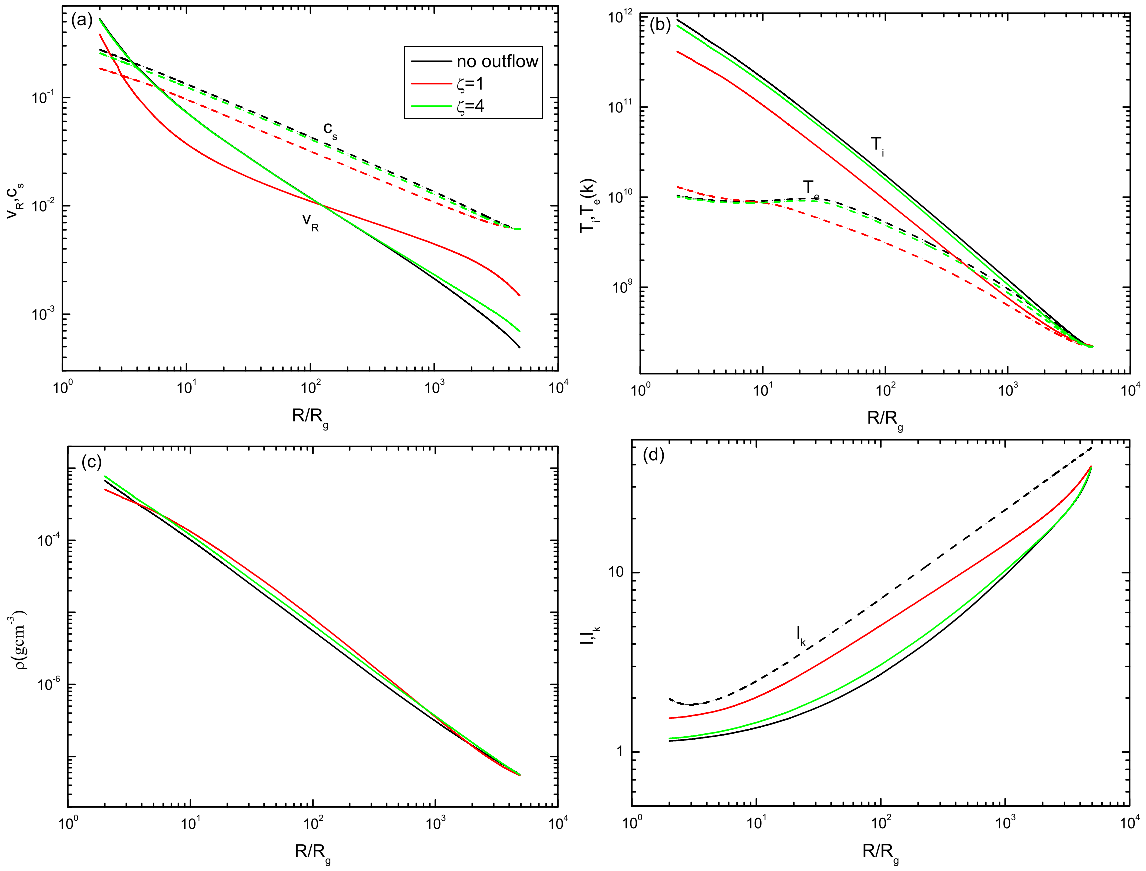

Figure 5. The same as Fig. 2, but the accretion rate at the outer radius $\dot{m}_0 = 10^{-2}$, and $\beta = 0.925$, are adopted.

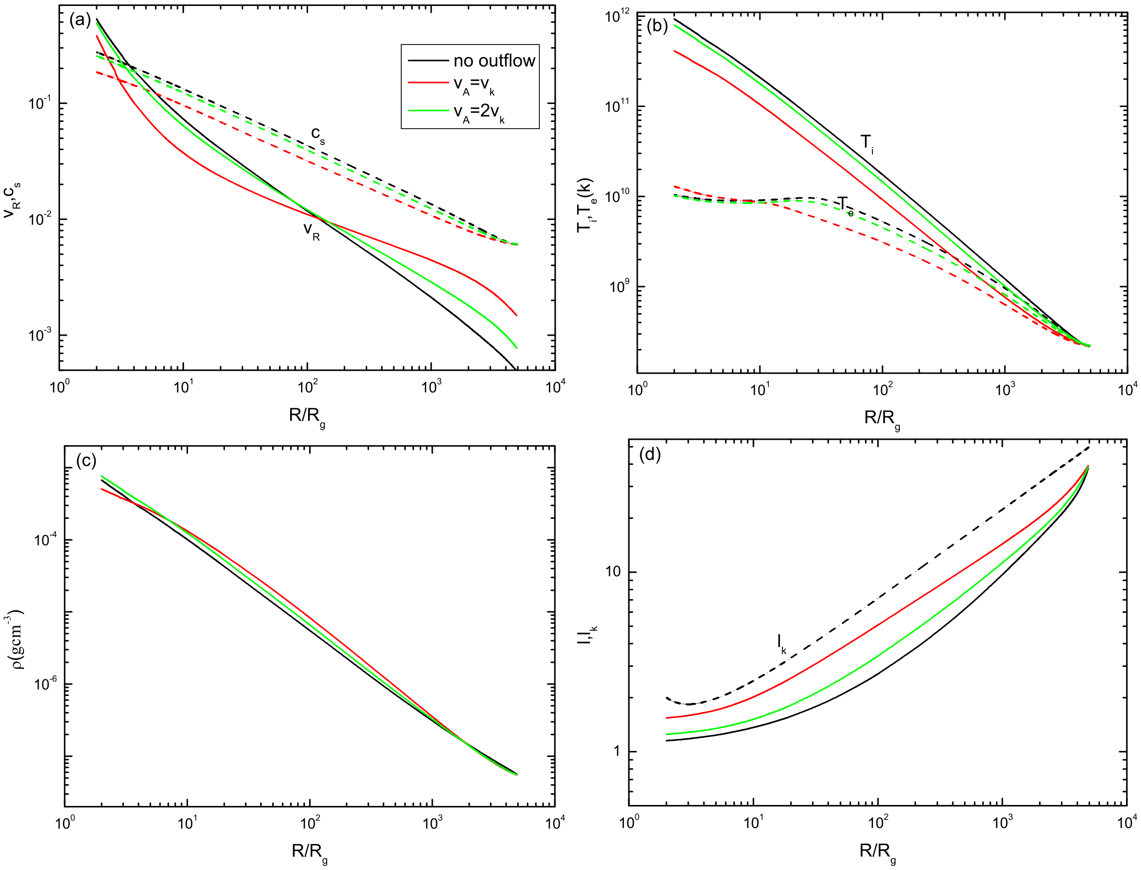

Figure 6. The same as Fig. 3, but the accretion rate at the outer radius $\dot{m}_0 = 10^{-2}$, and $\beta = 0.925$, are adopted.

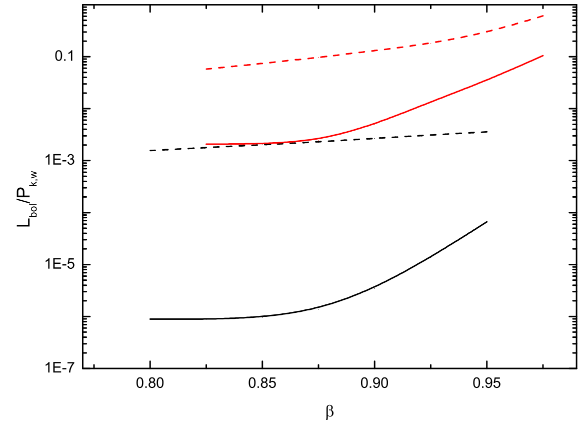

Figure 7. The ratio of the bolometric luminosity of accretion disc to the kinetic power of outflows for different values of β ($v_{\rm A} = v_{\rm k}$ is adopted). The black lines and red lines are for the accretion rate at the outer radius $\dot{m}_0 = 10^{-5}$ and 10^{-2} respectively, while the solid lines and dashed lines correspond to $\zeta = 1$ and 4 respectively.